Stem Cell Research (2014) 13, 465–477

Available online at www.sciencedirect.com

ScienceDirect

www.elsevier.com/locate/scr

CD34/CD133 enriched bone marrow progenitor cells promote neovascularization of tissue engineered constructs *in vivo*

Marietta Herrmann, Andreas Binder, Ursula Menzel, Stephan Zeiter, Mauro Alini, Sophie Verrier*

AO Research Institute Davos, Clavadelerstrasse 8, 7270 Davos, Switzerland

Received 23 January 2014; received in revised form 22 August 2014; accepted 13 October 2014
Available online 22 October 2014

Abstract Vascularization is critical for 3D tissue engineered constructs. In large size implants the ingrowth of vessels often fails. The purpose of this study was to identify an easily accessible, clinically relevant cell source able to promote neovascularization in engineered implants *in vivo* and to establish an autologous culture method for these cells.

MSCs (mesenchymal stem cells) and an endothelial progenitor containing cell (EPCC) population were obtained from human bone marrow aspirates. The expression of endothelial-markers, uptake of acetylated low density lipoprotein (acLDL) and tube-like structure formation capability of EPCCs were analyzed after expansion in endothelial growth medium or medium supplemented with autologous platelet lysate (PL). EPCCs were co-seeded with MSCs on hydroxyapatite-containing polyurethane scaffolds and then implanted subcutaneously in nude mice.

Human EPCCs displayed typical characteristics of endothelial cells including uptake of acLDL and formation of tube-like structures on Matrigel™. *In vivo,* EPCCs cultured with PL triggered neovascularization. MSC/EPCC interactions promoted the maturation of newly formed luminal structures, which were detected deep within the scaffold and partly perfused, demonstrating a connection with the host vascular system.

We demonstrate that this population of cells, isolated in a clinically relevant manner and cultured with autologous growth factors readily promoted neovascularization in tissue engineered constructs *in vivo* enabling a potential translation into the clinic.

Abbreviations: AAALAC, Association for Assessment and Accreditation of Laboratory Animal Care international; acLDL, Acetylated low density lipoprotein; BM, Bone marrow; CEPC, Circulating EPC; EC, Endothelial cell; EPC, Endothelial progenitor cell; EPCC, Endothelial progenitor containing cell population; FACS, Fluorescence activated cell sorting; HA, Hydroxyapatite; HUVEC, Human umbilical vein endothelial cell; MACS, Magnetic associated cell sorting; MNC, Mononuclear cells; PDGF, Platelet derived growth factor; PL, Platelet lysate; PRP, Platelet rich plasma; PU, Polyurethane; RANTES, Regulated on activation, normal T cell expressed and secreted; RT, Room temperature; SEM, Standard error of the mean; VEGF, Vascular endothelial growth factor

* Corresponding author. Fax: +41 814142288.
E-mail addresses: Marietta.herrmann@aofoundation.org (M. Herrmann), andreas.binder@stud.uni-regensburg.de (A. Binder), Ursula.menzel@aofoundation.org (U. Menzel), Stephan.zeiter@aofoundation.org (S. Zeiter), Mauro.alini@aofoundation.org (M. Alini), sophie.verrier@aofoundation.org (S. Verrier).

http://dx.doi.org/10.1016/j.scr.2014.10.005

Introduction

Vascularization is essential in tissue engineering approaches. This is evident by the limited diffusion distance of oxygen from blood vessels into surrounding tissue, which ranges between 150 and 200 μm (Folkman and Hochberg, 1973). Auger et al. reported that a tissue engineered construct exceeding a size of 400 μm in any dimension has to be vascularized in order to guarantee a sufficient supply of oxygen and nutrients to cells as well as the clearance of metabolic products (Auger et al., 2013). Vascularization is of particular importance for the engineering of highly vascularized tissues, such as bone (Laroche, 2002). It has been shown that angiogenesis is crucial to enable bone repair (Carano and Filvaroff, 2003; Das and Botchwey, 2011) as well as in bone tissue engineering of constructs of clinically relevant size (Griffith and Naughton, 2002). Indications for the clinical use of tissue engineered constructs are given in cases of critical size defects and non-unions (Fayaz et al., 2011).

Previous studies have shown that the ingrowth of vessels into grafts is not rapid enough to ensure cell survival (Auger et al., 2013; Laschke et al., 2006), where re-population of scaffolds with host endothelial cells (ECs) may take up to 14 days (Tremblay et al., 2005). In contrast, inosculation of pre-formed tubular structures or micro-vessels could be observed within 2–4 days (Tremblay et al., 2005; Laschke et al., 2009). Consequently, many recent tissue engineering approaches have focused on the *in vitro* pre-vascularization of grafts by the addition of ECs (Rouwkema et al., 2006; Fuchs et al., 2009; Henrich et al., 2009; Pang et al., 2013; Yu et al., 2008; Duttenhoefer et al., 2013). Various cell types have been used as source of ECs. Mature ECs such as human umbilical vein endothelial cells (HUVECs) or human dermal microvascular ECs promoted vascularization of tissue engineered constructs in animal models (Koob et al., 2011; Thein-Han and Xu, 2013). However, the availability and proliferation capacity of these cells are limited and extensive and time-consuming *in vitro* amplification is required (Auger et al., 2013). Adipose tissue stromal microvascular fractions have also been shown to be a source of ECs (Planat-Benard et al., 2004; Scherberich et al., 2007). Other tissue engineering approaches focus on endothelial progenitor cells (EPCs). Asahara et al. were the first to isolate EPCs from peripheral blood mononuclear cells (Asahara et al., 1997). EPCs originate from the hematopoietic lineage (Masuda and Asahara, 2003) and have significantly higher long-term proliferation capabilities than mature ECs (Lin et al., 2000). Circulating EPCs (CEPCs) are mobilized from the bone marrow (BM) niche (Asahara et al., 1999). Two subtypes of CEPCs have been described and termed early and late outgrowth ECs according to the appearance of colonies after seeding mononuclear cells on fibronectin coated plates (Lin et al., 2000; Kalka et al., 2000). Besides, various approaches have been focused on the direct selection of the hematopoietic progenitors by FACS or MACS and subsequent differentiation of cells towards an EC phenotype by supplementation of angiogenic growth factors. These isolation and enrichment strategies have mostly focused on the surface markers CD34, CD133 and vascular endothelial growth factor receptor 2 (VEGFR2, also KDR or CD309) (Masuda and Asahara, 2003; Yin et al., 1997; Peichev et al., 2000). However, the phenotypic characterization of EPCs remains difficult and is dependent upon species, cell source and *in vitro* culture conditions (Timmermans et al., 2009; Critser et al., 2011). EPCs are typically characterized by their ability to bind lectin from *Ulex europaeus* and to take up acetylated low density lipoproteins (acLDL) (Rafii et al., 1994). None of these widely used criteria are specific to ECs, and do not allow them to be distinguished from hematopoietic cells, which has led to a debate about the true nature of the various hematopoietic cell populations referred to as EPCs (Timmermans et al., 2009; Yoder et al., 2007; Mund et al., 2012). In contrast to the unclear identity of those cells their angiogenic potential has been readily shown in various preclinical and clinical studies (Krenning et al., 2009).

The expansion and maturation of mature ECs and EPCs requires the addition of pro-angiogenic growth factors such as VEGF. With regards the translation of cell-based therapies into clinic, it is of interest to avoid the expensive and controversial use of recombinant growth factors. The supplementation of growth medium with platelet lysate (PL) containing autologous growth factors represents a promising alternative. PL has already been used to supplement cultures of MSCs (Verrier et al., 2010). Recent work from our group has shown that EPCs can be expanded with PL (Lippross et al., 2011). Furthermore, EPCs grown in PL-containing medium induced tube-formation in 3D co-cultures with MSCs after 1 week of *in vitro* culture (Duttenhoefer et al., 2013).

The current study aimed to enrich a human endothelial progenitor containing cell (EPCC) population and to investigate (i) its potential to differentiate towards mature ECs and (ii) to promote neovascularization *in vivo*. The emphasis was to establish an autologous culture method using PL to facilitate the translation into clinic.

Material and methods

Preparation and characterization of platelet lysate (PL) and platelet rich plasma (PRP)

PL was produced as previously described (Lippross et al., 2011). In brief, platelet concentrates (5× above physiological concentration) were obtained by platelet aphaeresis (Kantonspital Graubünden). After centrifugation, the pellet was resuspended in half of the original volume using phosphate buffered saline (PBS, Sigma). PL was washed with PBS and activated by sonication for 15 min followed by freezing at −20 °C. Prior to use, PL was thawed and centrifuged to eliminate remaining platelet debris, subsequently the supernatant was used. PRP was also prepared from platelet concentrates. After centrifugation at 2000*g* for 20 min the pellet was resuspended in the supernatant (1/10 original volume), resulting in a final 50× enrichment of platelets compared to the physiological density. The PRP was activated by sonication for 15 min and freezing at −20 °C. PL and PRP samples (n = 3) were pooled from three different platelet concentrates and randomly matched to normalize any donor specific influences.

The presence of angiogenic growth factors in PL (pooled samples, n = 3) was examined using a human angiogenesis protein array (C-series1000, RayBio). PL (1 ml/membrane) was incubated for 60 min with the array membranes. Signal detection was performed according to the manufacturer's protocol. Chemiluminescence was detected after 25 min of

exposure with a ChemiGenio Bio Imaging System (Syngene). Semi-quantification was performed by averaging values from duplicated spots and measuring pixel intensity using ImageJ (Rasband, NIH). Data are presented as relative abundance in comparison to positive control on the membranes.

BM derived mononuclear cell (MNC) isolation and MSC culture

BM aspirates in citrate phosphate dextrose adenine-containing S-monovettes (Sarstedt) were obtained from iliac crest or vertebra of patients (Suppl. Table 1) undergoing routine orthopedic surgery after informed consent and approval by the local ethic committees (KEK Bern 126/03). BM aspirates were diluted 1:4 with PBS and layered onto Ficoll (Histopaque-1077, Sigma) and centrifuged at 800*g* for 20 min at room temperature. The MNC interphase was collected, washed with αMEM (Gibco) containing PenStrep (100 U/ml, Gibco), 10% fetal bovine serum (FBS, Gibco) followed by 15 min centrifugation at 400*g*. MNCs were seeded at the density of 5×10^4 cells per cm^2 with αMEM containing 10% FBS, PenStrep (100 U/ml) and 5 ng/ml bFGF (R&D Systems). After 4 days, non-adherent cells were removed and monolayer selected MSCs expanded with medium changes every 3 days. When 80% confluency was reached cells were detached using 0.5% trypsin-EDTA (Gibco) and reseeded at a density of 3×10^3 cells/cm^2. All experiments were performed with cells between passages 2 and 3.

EPCC enrichment and culture

Freshly isolated MNCs were centrifuged at 300*g* for 10 min and resuspended in PBS with 0.5% bovine serum albumin (Sigma) and 2 mM EDTA (Sigma). Cells were enriched using the MiniMACS Magnetic Microbead System (Miltenyi Biotec) sequentially using CD34 and CD133 specific antibodies according to the manufacturer's instructions, the obtained cell population is referred to as an endothelial progenitor containing cell population (EPCC). EPCCs were seeded at a density of 5×10^4cells/cm^2 in six-well plates and cultured in either EBM-2 medium (Lonza) with full growth factor supplementation supplied by the EGM-2 kit (Lonza), referred to as EGM, or Iscove's Modified Dulbecco's Medium (IMDM, Gibco) containing FBS (Gibco), PenStrep (100 U/ml), 1% NEAA (Gibco) and PL. A combination of 2% FBS–8% PL or 5% FBS–5% PL was used. The first medium change was performed after 4 days, with subsequent medium changes every 3 days. Cells were subcultured upon 80% confluency and after trypsinization reseeded at a density of 5×10^3 cells/cm^2. HUVECs (Gibco) were grown on plates coated with Quick Coating (AngioProteomic) in EGM.

Characterization of EPCCs

Cells were analyzed for expression of endothelial marker by flow cytometry. For immunolabeling $1–2 \times 10^5$ cells were stained with the following antibodies alone or in different combinations: CD34-FITC, CD34-PE, CD133-APC, CD309-PE (Miltenyi Biotech), CD31-AlexaFluor680 (BD Bioscience) and goat anti mouse IgG isotype control-APC (BD Bioscience) and incubated for 30 min on ice according to the manufacturer's recommendations. Cells were washed in PBS before analysis using a BD FACS Aria III (BD Bioscience). At least 25,000 events were recorded per sample and a gating strategy used to exclude cell doublets.

To analyze the uptake of acLDL, 5×10^5 cells were seeded in six-well culture plates and left overnight. Cells were then incubated with 1 μg/ml Dil-labeled acLDL (Life Technologies) for 4 h at 37 °C. Subsequently, cells were washed 3× with PBS, detached and cell-associated fluorescence measured by flow cytometry.

To study the ability of cells to form tube-like structures, we seeded 3×10^4 cells in two-well Nunc Lab-Tek™ Chamber Slides (Thermo Scientific) coated with a thin layer of Matrigel™ (growth factor reduced, BD Bioscience) and incubated in the same media that the cells had previously been cultured in. Formation of tube-like structures was observed using a Axiovert40 CFL microscope (Zeiss) 0.5 h, 6 h and 24 h after seeding and incubation at 37 °C. For quantitative analysis images from three fields of view were taken from each well at 5× magnification and total tube length measured using Axiovision software (Zeiss).

In vivo model of neovascularization in tissue engineered constructs

The *in vivo* study was approved by the ethical committee of the canton of Grisons in Switzerland. All procedures were performed in an AAALAC approved facility and according to Swiss animal protection law and regulations. Bioresorbable elastomeric polyurethane scaffolds (diameter 8 mm, thickness 2 mm) containing nanoparticles of hydroxyapatite (PU-HA), porosity 200–600 μm were cut in half (half-moon scaffolds). Before cell-seeding, scaffolds were incubated in IMDM medium and degassed for 1 h. 1.5×10^6 MSCs and/or EPCCs (expanded in IMDM with 5% FBS–5% PL) were resuspended in 50 μl PRP, mixed with 8 μl of a thrombin solution (50U/ml, Baxter) and immediately seeded into the scaffolds. The following combinations of cells were used: 100% MSC, 100% EPCC, 75% EPCC + 25% MSC, 50% EPCC + 50% MSC (n = 5). Control scaffolds were seeded with PRP alone or left untreated (n = 2). Scaffolds were either pre-cultured for 1 week in IMDM supplemented with 7.5% FBS, 2.5% PL, PenStrep (100 U/ml), 1% NEAA, 5 mM β-glycerophosphate, 50 μM ascorbic acid, 10^{-8} M dexamethasone and aprotinin (500 U/ml, Sigma) or used directly for implantation in 9-week-old female specific pathogen free CD1-nude mice (Charles River). Two scaffolds were implanted subcutaneously in each mouse. Mice were anaesthetized by exposure to isoflurane. Buprenorphine (0.1 mg/kg) was administered subcutaneously before the start of the surgery. After preparation of the surgical area for aseptic surgical intervention, two separate 1 cm skin incisions were made in the dorsal midline over the thoracic spine. At each incision, a pocket was prepared by blunt subcutaneous preparation to one side of the thorax. One scaffold was then placed into each pocket and the surgical incision was closed with 5–0 Vicryl rapid (Ethicon). Following surgery, acetaminophen was added to the drinking water for 3 days (200 mg/100 ml; UPSAMEDICA GmbH). Mice were housed in individually ventilated cages within a barrier throughout the study and fed ad libitum ("Alleinfuttermittel für Mäuse," Art. 3436; Kliba) with free access to drinking water. After 8 weeks the mice were

euthanized by cervical dislocation, the scaffolds were excised and fixed in 70% methanol. To evaluate anastomosis of the implants two mice per group received an intravenous injection of 20 mg/kg FITC-labeled lectin from *U. europaeus* (Sigma) 1 h prior to euthanasia.

Immunohistochemistry

Fixed scaffolds were cut in half. One half was incubated in 1% sucrose in PBS overnight, frozen in tissue freezing medium (Leica) and 10 μm thick cryosections were prepared. For immunohistochemistry sections were rehydrated for 10 min in deionized water, blocked for 60 min with 5% goat serum (Vector Laboratories) and incubated for 60 min with rabbit-anti human α smooth muscle actin (αSMA) antibody (Abcam). After washing sections were incubated for 30 min with TRITC-labeled goat-anti-rabbit secondary antibody (Abcam). Sections were washed and mounted using Prolong Gold Antifade reagent containing DAPI (Life Technologies). Microscopic analysis was performed using an Axiovert 200m microscope equipped with an AxiocamHRc and Axiovision software (Zeiss). A montage of the entire cross section of the scaffold was assembled from individual images at 10× magnification using the Mosaix tool. Regions of interest (ROIs) were defined as (i) the whole cross-section area (16 mm^2) and (ii) the center of the scaffold (8.6 mm^2). Cell content within the ROIs was estimated by determination of the DAPI covered area. Calculations were made using KS software (Zeiss) and a custom made Macro in Excel (Microsoft). The number of αSMA positive vessels was counted manually and their penetration depth measured using Axiovision software. Total vessel number was normalized to the size of the section of the scaffold to account for slight differences in scaffold size.

The second half of each scaffold was embedded in Methylmethacrylate (MMA). Fixed scaffolds were dehydrated in a series of graded alcohols. The ethanol was cleared from the samples by immersion in xylene (Siegfried) for 6–8 h. Samples were embedded in MMA according to manufacturer's instructions (Sigma-Aldrich). The samples polymerized within 5–10 days. Polymerized samples were cut with a Leica SP1600 saw microtome (Leica) to 80–100 μm thick sections, mounted on opaque Plexiglas slides (Seamdeni) and imaged using an Axioplan2 fluorescence microscope equipped with an AxioCamHRc camera and AxioVision software V3.1 (Zeiss).

Statistics

Statistical analysis of data was performed using Prism software (GraphPad). Data were tested for normal distribution and one-way ANOVA with Tukey's multiple comparison test was applied to test for significant differences between experimental groups. Data presented are means ± standard error of the mean (SEM) unless stated otherwise.

Results

Abundance of CD34/CD133+ cells in human BM aspirates

Human BM MNCs were characterized by flow cytometry. Fig. 1(A) shows a representative forward–side scatter profile of MNC. We focused on the region P1, containing cells with low granularity including lymphocytes as well as stem and progenitor cells and examined the expression of CD34, CD133 and CD309 (Fig. 1B and Suppl. Table 1). CD34+ cells accounted for 10.9 ± 4.7% of agranular MNC. A smaller population of CD133+ cells was detected (0.6 ± 0.5%). Of the CD34+ cells, two distinct populations could be distinguished, low level ($CD34^{low}$) or high level ($CD34^{high}$). Interestingly, all CD133+ cells were also positive for $CD34^{high}$ (Fig. 1B, C), The expression of CD309 was low (1.1 ± 1.6%, Suppl. Table 1). As shown in Fig. 1(D, E) we could exclude a correlation between the abundance of CD34/CD133+ cells and the age or gender of donors.

Human BM-derived EPCCs display characteristics of mature ECs

Following enrichment using MACS® 68.1 ± 20.7% of cells were CD34+, 60 ± 18.5% expressed high level of CD34 and 14.3 ± 5.2% were CD34/CD133+ (Fig. 2A, B).

After monolayer expansion of EPCCs the initial expression of CD34 and CD133 was nearly completely lost (not shown). At this stage we analyzed EPCCs with regard to typical EC properties and compared them to HUVECs. Firstly, we evaluated expression of CD31, expressed on mature ECs and show that HUVECs are nearly 100% positive for CD31, while EPCCs in passages 2 and 3 do not express CD31 when cultured in EGM (Fig. 2C, Suppl. Fig. 1). Secondly, we studied the ability of cells to take up acLDL. Analysis of cell-associated fluorescence by flow cytometry showed that both EPCCs and HUVECs efficiently took up acLDL (Fig. 2D), with an average of 82.9 ± 12.0% and 99.5 ± 0.2% positive EPCCs and HUVECs, respectively.

The capability of EPCCs and HUVECs to form tube-like structures was examined on Matrigel™. For both cell types the formation of tube-like structures was evident after 6 h (Fig. 2E). After 24 h, a complex network of tube-like structures could be observed (Fig. 2E). The efficiency of tube-like structure formation was assessed by the total tube length after 24 h showing EPCCs are as efficient as HUVECs (Fig. 2F). In addition, we show that EPCCs retained all endothelial characteristics when further expanded for another passage (Suppl. Fig. 1).

Expansion of human BM-derived EPCCs with PL preserves endothelial characteristics

To establish an autologous culture method for EPCCs, we used PL as a medium supplement instead of recombinant angiogenic factors. As the composition of PL is still poorly understood we performed a screening array to identify the most abundant growth factors. In total, 11 out of 43 factors were detected in PL (Fig. 3). Most abundant were the pro-angiogenic factors RANTES (CCL5), epidermal growth factor (EGF) and GRO (constituting CXCL1, CXCL2 and CXCL3 chemokines). Further pro-angiogenic factors including angipoietin-1, ENA-78 (CXCL5), angiogenin, platelet-derived growth factor BB (PDGF-BB) and transforming growth factor beta (TGFβ) could be detected at lower levels. Three anti-angiogenic factors were identified at low

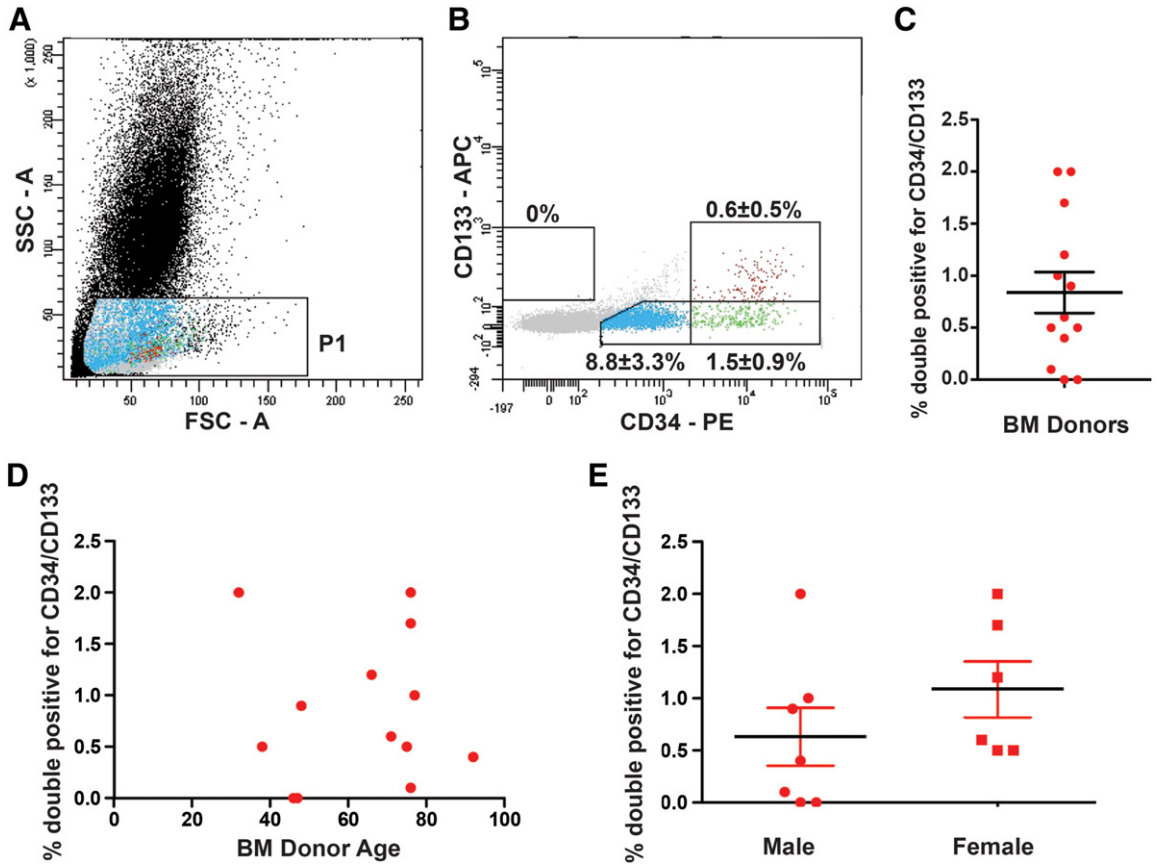

Figure 1 Abundance of CD34/CD133+ cells in human BM aspirates. Flow cytometry analysis of mononuclear cell fractions (MNC) obtained by density centrifugation of human BM. A. Representative profile of MNCs in respect of size (FSC) and granularity (SSC). P1 contains cells with low granularity including stem- and progenitor cells. B. Staining of CD34 (x-axis) reveals two cell population expressing either low or high level of CD34. Staining of CD133 (y-axis) shows a small, population of CD34/CD133+ cells. C. Donor variation of CD34/CD133+ cells. D, E. Correlation of CD34/CD133+ cells with age (D) and sex (E) of donors. n = 13. Error bars depict the SEM.

levels: tissue inhibitor of metalloproteinases 1 (TIMP-1), TIMP-2 and endostatin.

Further, we studied the endothelial characteristics of EPCCs grown in IMDM containing 2% FCS–8% PL (IMDM2-8) or 5% FCS–5% PL (IMDM5-5). CD31 was expressed by 31.6 ± 13.85% and 41.0 ± 5.7% of cells grown in IMDM5-5 or IMDM2-8, respectively (Fig. 4A). The percentage of CD31+ cells was higher in these media conditions when compared to EPCCs grown in EGM (Fig. 2C). The uptake of acLDL was significantly higher in EPCCs expanded in IMDM2-8 than in IMDM5-5: 47.6 ± 10.8% vs. 16.5 ± 6.2% ($p < 0.05$, Fig. 4B).

On Matrigel™ EPCCs grown with autologous growth medium showed only a minor capability to form tube-like structures (Fig. 4C). In comparison to the complex tubular network shown by EPCCs cultured in EGM (Fig. 2), here only short tube-like structures could be detected after 24 h of incubation resulting in a much lower total tube length: 5.1 ± 2.0 mm were measured with IMDM5-5 and 10.5 ± 1.9 mm with IMDM2-8 (Fig. 4D), while 21.0 ± 7.6 mm could be observed for EPCCs cultured in presence of EGM (Fig. 2F).

Comparable results were obtained for EPCCs grown for another passage in the individual growth medium (Suppl. Fig. 1).

EPCCs promote neovascularization *in vivo*

To study the potential of EPCCs to trigger neovascularization *in vivo* we implanted PU-HA scaffolds pre-seeded with different proportions of MSCs and/or EPCCs in presence of PRP subcutaneously in nude mice (Fig. 5A). Immunofluorescence staining αSMA detected capillary-like structures in all scaffolds. Fig. 5(B, C) shows representative images of scaffolds seeded with EPCCs alone implanted directly (Fig. 5B) or seeded with a 1:1 mixture of EPCCs and MSCs and implanted after 1-week of pre-culture (Fig. 5C). To address the question whether the observed vessels were connected with the host vascular system, FITC-lectin was intravenously injected before euthanasia of mice. FITC staining could be detected in vessels within the implants (Fig. 5D–F), showing that newly formed vessels were connected to the circulation of the host mice.

Cell content, vessel number and their location were quantified. As illustrated in Fig. 6A the sections were taken in the center of the scaffold (dashed line, Fig. 6A(i)). We assessed the whole cross-section of the scaffolds (Fig. 6A(ii), plain line) as well as the center of the scaffolds (Fig. 6A(ii), dashed line). Fig. 6(B–D) illustrates the results for directly implanted scaffolds. Cells were detected in all cell-seeded

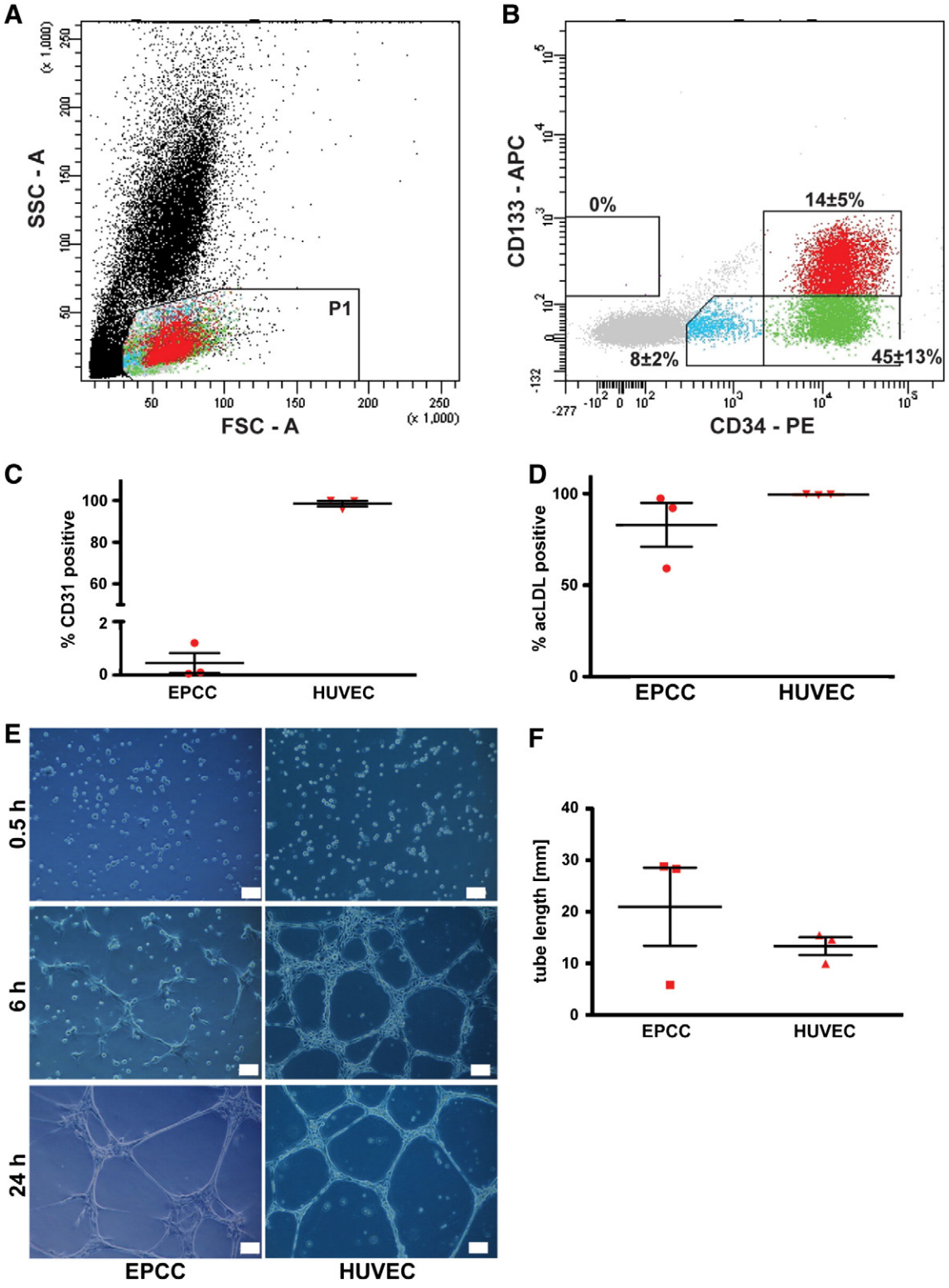

Figure 2 Human BM-derived EPCCs display characteristics of mature ECs. EPCCs were enriched from MNCs using CD34 and CD133 MACS® microbeads. A. Flow cytometry analysis of the enriched cell population. Representative profile of MNC in respect of size (FSC) and granularity (SSC). Region P1 contains cells with low granularity including stem- and progenitor cells. B. Double staining for CD34 and CD133 demonstrates enrichment of high expressing CD34 cells and CD34/CD133+ cells. C. CD31 expression on EPCCs expanded in EGM (passage 2) and HUVECs evaluated by flow cytometry. Only HUVECs did express CD31. D. Uptake of Dil-labeled acLDL particles, assessed by flow cytometry, was seen in both EPCCs and HUVECs. E. Representative image of EPCCs (left panel) and HUVECs (right panel) incubated on growth factor reduced Matrigel™. Scale bars = 100 μm. F. Quantification of the length of tube-like structures, given values are averages obtained from analyzing three optical fields. In all graphs single values are shown as individual dots and the mean with SEM is depicted, n = 3.

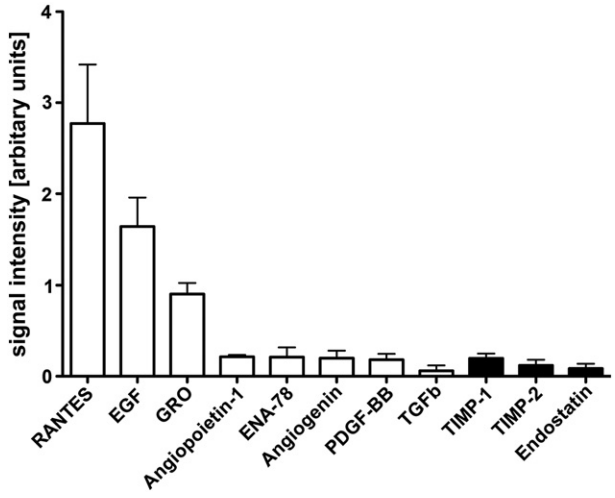

Figure 3 Platelet-lysate as source of pro-angiogenic factors. PL preparations from three donors were pooled and the relative abundance of angiogenic factors was analyzed by protein antibody array. Values are given as signal intensity in comparison to an internal positive control. Bars depict mean values with SEM, white bars show pro-angiogenic factors, black bars indicate anti-angiogenic factors, n = 3 (referring to three pooled samples).

scaffolds, with 2.5–3.9% of the total cross sectional area (Fig. 6B, open bars). In contrast, cell-free scaffolds showed a lower cell content representing 1.2% and 2.3% of the total cross sectional area. In the center of scaffolds, no variation could be detected between the different experimental groups with regards to cell content, range 0.6–1.5% of the total area (Fig. 6C, open bars).

Vascular structures were identified in all experimental groups throughout the entire scaffold (Fig. 6B, blue bars). However, comparing vascular ingrowth into the center of the scaffolds (Fig. 6C), the number of vessels varied depending upon the combination of cell types seeded. In directly implanted scaffolds the vessel number was directly related to the number of EPCCs, although these differences did not reach statistically significance because of huge variations between individual scaffolds (Fig. 6C, blue bars). We also analyzed the penetration depth of individual vessels into the scaffolds. Compared to cell-free PU-HA scaffolds (140 ± 16 μm) a significant higher mean penetration was observed with 100% EPCC (216 ± 10 μm, $p < 0.01$) and with 75% EPCC + 25% MSC (203 ± 12 μm, $p < 0.05$, Fig. 6D).

Overall, pre-cultured scaffolds showed a slightly lower cell content than directly implanted scaffolds, ranging between 1.6% and 2.3% of the total area (Fig. 7A, open bars). Similar numbers were detected in the center of scaffolds (Fig. 7B, open bars). The highest vessel number was detected in the center of scaffolds containing co-cultures of EPCCs and MSCs (Fig. 7B, blue bars): 2.4 ± 0.4 vessels in scaffolds seeded with 50% EPCC + 50% MSC ($p < 0.05$ in comparison to monocultures: 100% EPCC: 0.8 ± 0.2; 100% MSC 0.7 ± 0.3). The positive influence of MSC–EPCC co-cultures was also confirmed when we analyzed the penetration depth of vascular structures into the scaffolds (Fig. 7C). A significantly higher mean depth of 266 ± 15 μm was detected in scaffolds co-seeded with 50% MSC + 50% EPCC in comparison to 171 ± 11 μm for 100% MSC ($p < 0.001$) and 211 ± 10 μm for 100% EPCC ($p < 0.05$), which was also higher compared to directly implanted scaffolds (Fig. 6D).

Discussion

Human BM-derived EPCCs display similar angiogenic properties to HUVECs

In this study we demonstrate that BM-derived EPCCs promote neovascularization in tissue-engineered scaffolds. We show the abundance of a distinct population of CD34/CD133+ cells in human BM aspirate in all tested donors independent of age or gender. These cells contain a hematopoietic progenitor cell population bearing the potential to develop an EC phenotype when cultured in the presence of angiogenic growth factors (Peichev et al., 2000; Gehling et al., 2000; Quirici et al., 2001). Accordingly, various transplantation strategies to treat ischemic diseases have been focused on CD34+ cells (Kuroda et al., 2014). Interestingly, extensive work on circulating blood EPCs has revealed that the CD34+ CD133+ VEGFR2+ cell population failed to give rise to an EC population but formed hematopoietic colonies (Case et al., 2007). Work from the same group identified CD34+/CD45− cells as a putative EPC population and further studies showed that the cells express a combination of the EC marker CD34, CD31 and CD146 while CD133 and CD45 were absent (Case et al., 2007; Mund et al., 2012).

In the current study we enriched CD34/CD133+ cells using the MACS® microbeads system. Although the obtained cell population was not pure, MACS® enrichment presents a fast selection strategy requiring only minimal manipulation of cells which is of particular interest for clinical application. From a clinical point of view it is thought advantageous to work with a mixture of progenitor cells. Recent work has suggested that monocytic cells might also promote neovascularization (Shi et al., 2014).

We show that after an expansion EPCCs for two passages (~3 weeks) in angiogenic growth medium, cells had EC characteristics.

During the past years, many approaches have used various EPC populations to induce neovascularization in tissue-engineered scaffolds (Critser et al., 2011; Zisch, 2004; Johnson et al., 2011). EPCs have also been applied in the treatment of ischemic diseases (Krenning et al., 2009; Drela et al., 2012; Zhao et al., 2013). However, in the majority of these studies EPCs were derived from blood or even mature ECs were used. Such strategies require a time-consuming and expensive *in vitro* expansion because of a generally low yield of cells and/or limited proliferation potential. Blood outgrowth ECs appear as cobblestone-like cell colonies 4 weeks after cell isolation and then require further *in vitro* expansion (Kolbe et al., 2010). In contrast, we show that BM-derived EPCCs require a much shorter time of *in vitro* manipulation, namely colonies were present within a week after isolation. The superior proliferation potential of EPCCs from BM in comparison to blood-derived EPCs has also been reported by others (Muscari et al., 2010).

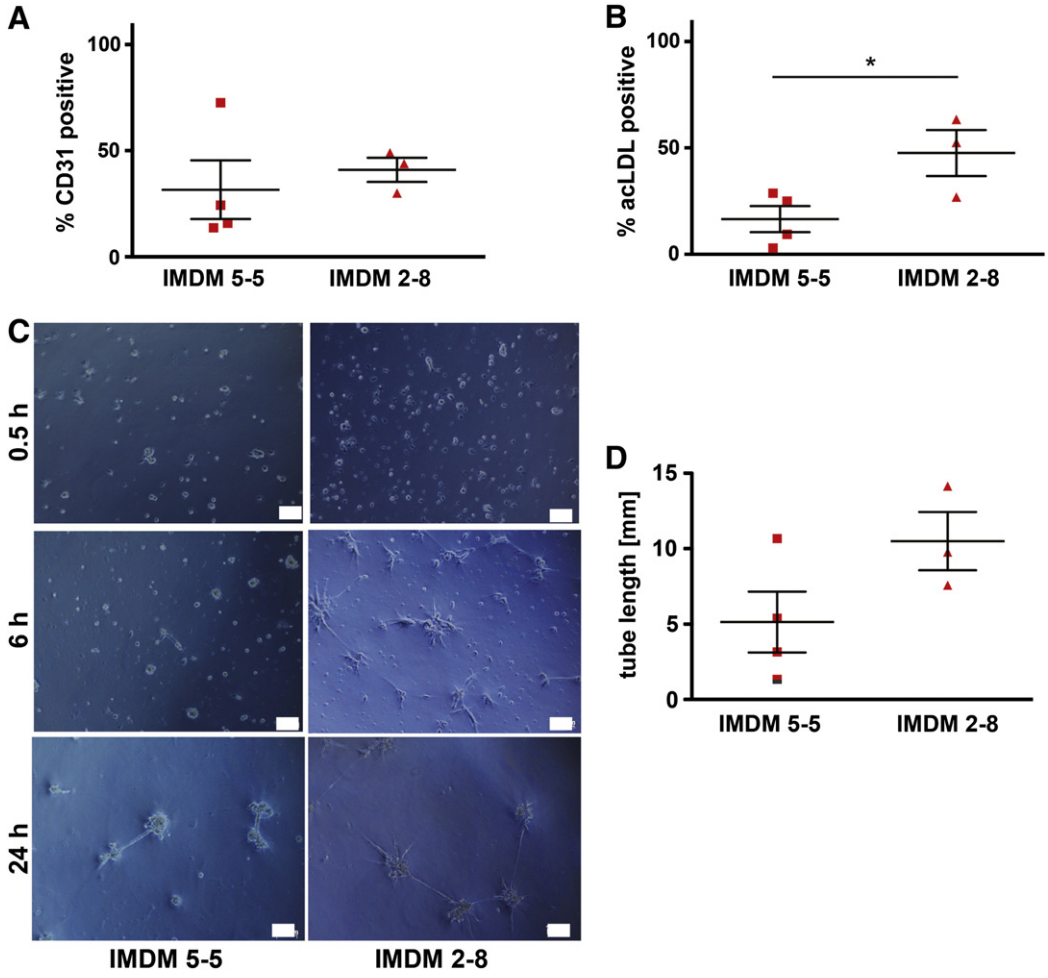

Figure 4 Expansion of human BM EPCCs with PL preserves endothelial characteristics. BM-derived EPCCs (passage 2) expanded in IMDM supplemented with autologous growth factors: IMDM with 5% FCS–5% PL (IMDM5-5) or 2% FCS–8% PL (IMDM2-8). A. Expression of CD31 evaluated by flow cytometry. B. Uptake of Dil-labeled acetylated LDL particles analyzed with FACS. C. Tube-like structure formation capability on Matrigel™. Scale bars = 100 μm. D. Quantification of total tube length, given values are average values obtained from analyzing three optical fields each. In all graphs single values are shown as individual dots and the mean with SEM is depicted, n = 3, *$p < 0.05$.

To assess the potential of human BM-derived EPCCs to function as mature ECs we first cultured these cells in EGM medium. Our results confirmed that EPCCs cultured in EGM have the same functional properties as mature HUVECs, demonstrated by their ability to take up acLDL and form tube-like structures on Matrigel™. In contrast, some recent *in vitro* studies have shown a limited endothelial potential of BM-derived EPCs. Amini et al. found that rabbit peripheral blood EPCs showed a higher expression of EC markers and a more pronounced ability to form tubular structures in Matrigel™ *in vitro* than BM-derived EPCs (Amini et al., 2012). Similarly, Chen et al. reported that mouse BM-derived EPCs failed to sprout in an *in vitro* 3D sprouting model (Chen et al., 2012). The different outcomes of these studies may be attributed to the fact that phenotypic characterization of EPCs depends on various factors including species, cell source and culture conditions (Timmermans et al., 2009). Studies analyzing EPCs of various species have shown that the selection and culture conditions may significantly impact proliferation, differentiation and maturation of these cells. Jianguo et al. reported that a combination of VEGF, bFGF, IGF and EGF was required for an optimized culture of porcine EPCs (Jianguo et al., 2010). Another study using porcine EPCs identified fibronectin-coating and VEGF as crucial factors to promote the endothelial properties of EPCs (Muscari et al., 2010). Interestingly, our data suggest that EPCCs cultured in EGM do not express CD31. Similar observations were made for *in vitro* amplified BM-derived EPCs from different species including rat, mouse and rabbit (Amini et al., 2012; Yang et al., 2011; Sekiguchi et al., 2011). However, the lack of CD31 expression at this point may be attributed to the *in vitro* monolayer culture and has no influence on the functional properties of EPCCs, demonstrated by the ability of EPCCs to form tube-like structures on Matrigel™.

In accordance with other studies, our data show that BM-derived EPCCs are highly efficient in promoting neovascularization *in vivo*. Similarly, Yu et al. demonstrated the potential of mouse BM-derived EPCs co-seeded with osteoblasts in a porous scaffold to induce capillarization in a segmental bone defect model (Yu et al., 2009). Another study

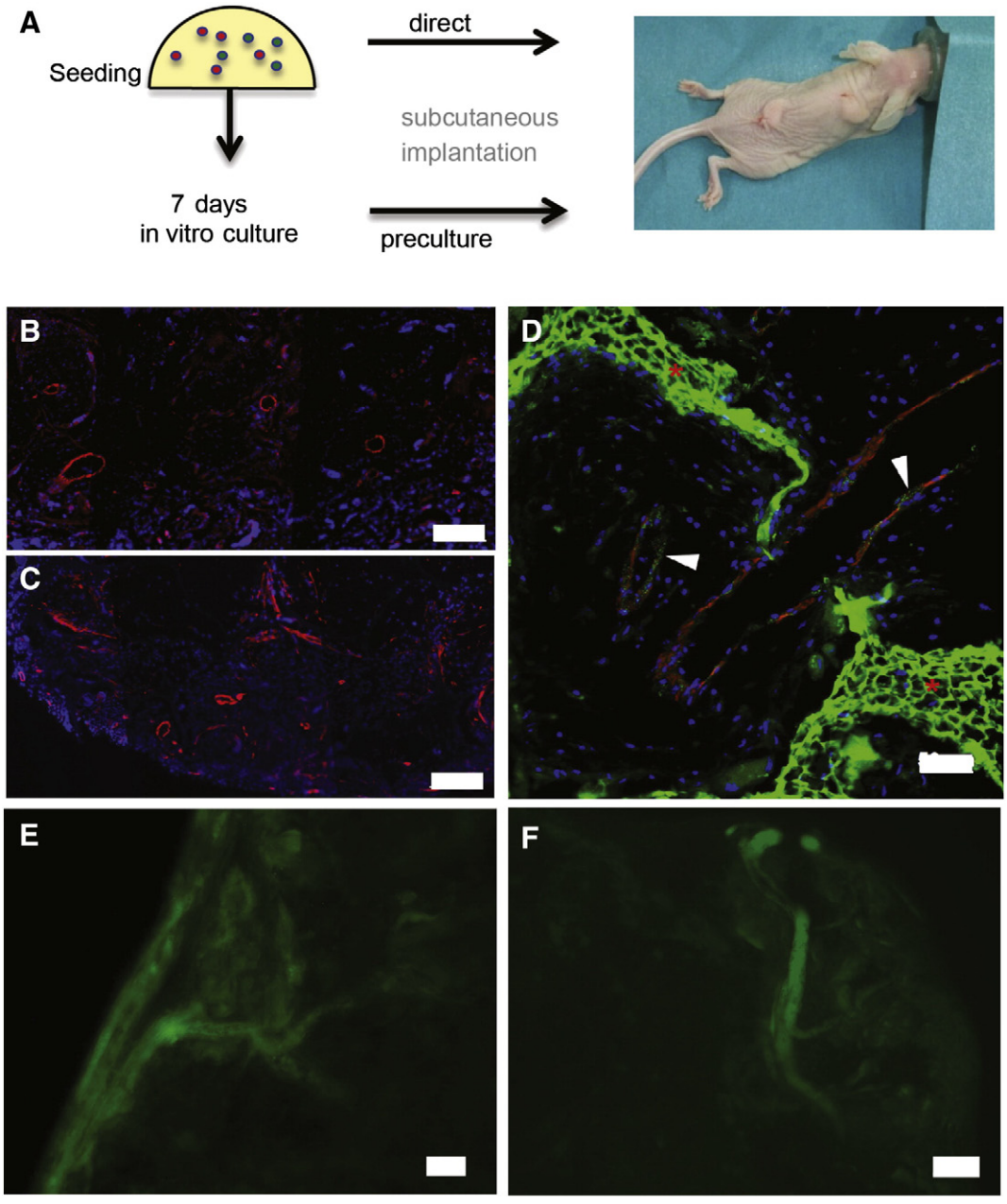

Figure 5 Neovascularization and anastomosis of vessels in subcutaneously implanted PU-HA scaffolds. A. PU-HA scaffolds were seeded with different proportions of EPCCs and MSCs in presence of PRP (n = 5). Empty scaffolds or scaffolds with PRP alone served as control (n = 2). Scaffolds were implanted subcutaneously into nude mice for 8 weeks. B–D. αSMA immunofluorescence staining (red) on cryosections detecting micro-vessels. Cell nuclei are stained with DAPI (blue). D-F. Detection of intravenously injected FITC-lectin (green) within micro-vessels on cryosections (D, green, arrowheads; asterisks = autofluorescence of the scaffold) and MMA-sections (E, F). Shown are representative images of a directly implanted scaffold seeded with 100% EPCCs (B, D) or 25% MSC + 75% EPCC (E.). C and F show images of scaffolds seeded with 50% MSC + 50% EPCC (C) or 25% MSC + 75% EPCC (F) and implanted after 7 days *in vitro* pre-culture. Scale bars depict 200 μm (B, C), 100 μm (F), 50 μm (D, E).

demonstrated the successful vascularization of MSC seeded porous β-tricalcium phosphate ceramic scaffolds in rabbits when BM-derived EPCs were added (Zhou et al., 2010). Zhang et al. observed that rabbit BM-derived EPCs were capable to generate a vascular network in osteogenic cell sheets (Zhang et al., 2012). Recently, Pang et al. showed that the addition of rabbit BM-derived EPCs to a demineralized bone matrix seeded with MSCs improved vascularization and healing of the defect *in vivo* (Pang et al., 2013).

Culture of EPCCs with autologous platelet-derived growth factors

We have previously reported that PL, containing autologous growth factors, boosts the expansion of EPCs *in vitro* (Lippross et al., 2011). In particular, the proliferation of EPCs was optimal in a medium containing 5% FCS and 5% PL. In addition, EPCs cultured with PL expressed endothelial markers such as angiopoitin 1, von Willebrand Factor (vWF),

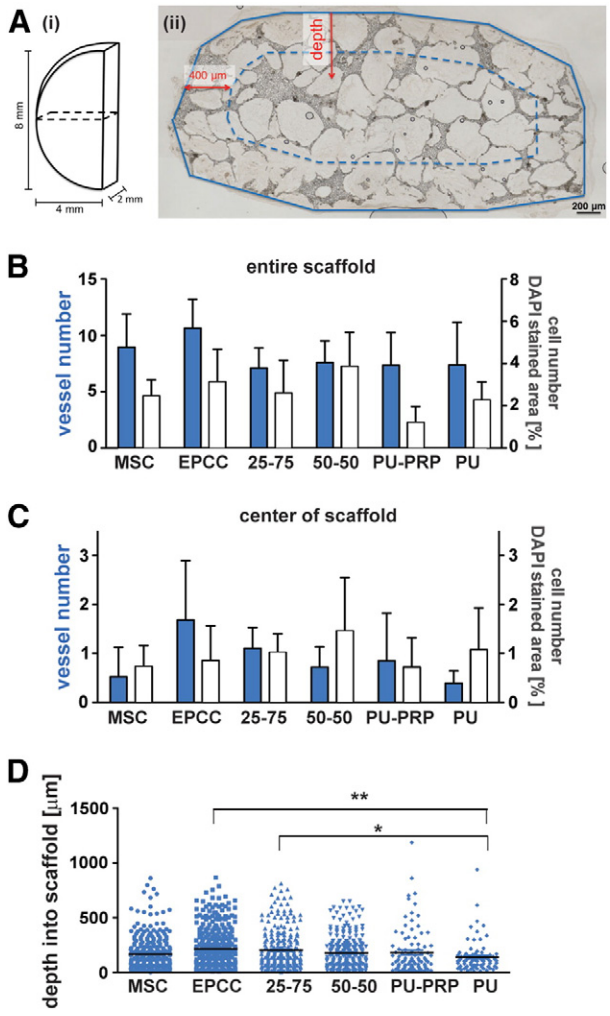

Figure 6 EPCCs promote neovascularization in directly implanted scaffolds *in vivo*. Quantitative analysis of vessel number and cell content in entire scaffolds (B) and in the center of scaffolds (C) as indicated in (A). Immunofluorescence staining for αSMA was performed as shown in Fig. 5 to detect blood vessels in directly implanted scaffolds. The cell content was estimated by measuring the area covered by DAPI nuclei staining. D. Depiction of the penetration depth of vessels, each dot corresponds to one vessel. N.B. the number of vessels in scaffold center was the highest in scaffolds with 100% EPCC. Bars depict mean values with SEM, n = 5 (cell-seeded scaffolds), n = 2 (cell-free scaffolds), *p < 0.05, **p < 0.01.

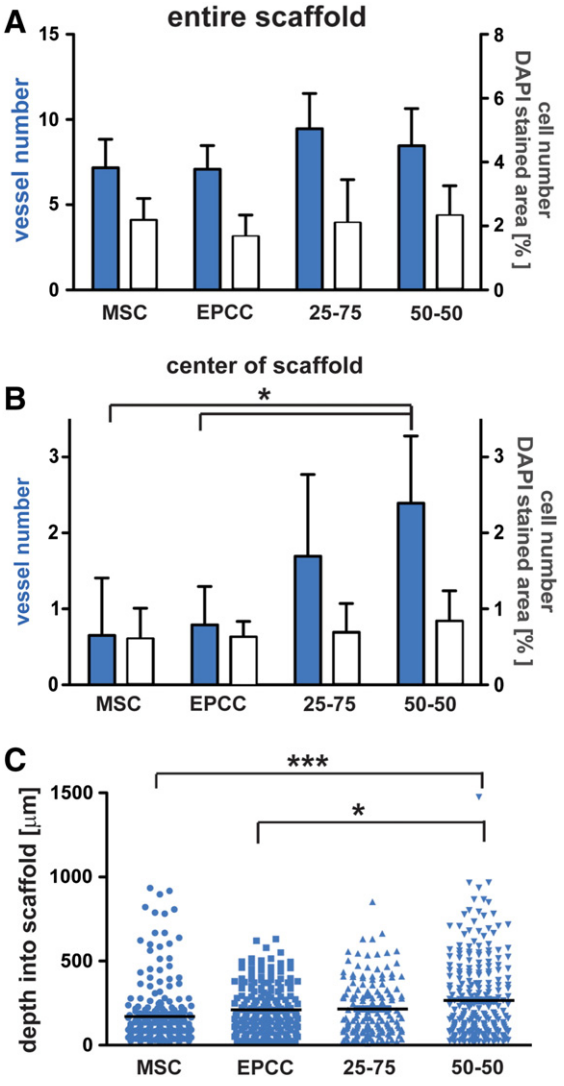

Figure 7 EPCC–MSC crosstalk is crucial for neovascularization in pre-cultured scaffolds.
Quantitative analysis of vessel number and cell content in entire scaffolds (A) and in the center of scaffolds (B). Immunofluorescence staining for αSMA was performed as shown in Fig. 5 to detect blood vessels in pre-cultured scaffolds. The cell content was estimated by measuring the area covered by DAPI nuclei staining. C. Depiction of the penetration depth of vessels, each dot corresponds to one vessel. N.B. the number of vessels in scaffold center was the highest in scaffolds with 50% MSC + 50% EPCC. Bars depict mean values with SEM, n = 5, *p < 0.05, ***p < 0.001.

PDGF-RB, TEK tyrosine kinase and CD31 and were able to build tube-like structures on Matrigel™, which was never observed with FBS alone (Lippross et al., 2011). This is in agreement with earlier studies having shown that platelets induce the differentiation of EPCs (Langer et al., 2007) and promote colony formation as well as migration of EPCs (Leshem-Lev et al., 2010).

To better understand the effect of PL on EPCCs, we analyzed PL with respect to its content of angiogenic factors. We found high levels of the pro-angiogenic factors RANTES, EGF and GRO (Suffee et al., 2012; Arenberg et al., 1997). A comparable profile was described by Fekete et al. reporting the expression of high levels of RANTES along with other pro-angiogenic factors including PDGF-AA, PDGF-AB/BB and TGFβ in human PL. This study also revealed the presence of GRO and bFGF (Fekete et al., 2012). In the current study we detected PDGF-BB and TGFβ only at minor levels, which might be attributed to the different activation method of the platelets or donor variability. Indeed high variation in growth factor content of different platelet preparations has been reported before (Lubkowska et al., 2012). In our study we could not detect VEGF, one of the most prominent pro-angiogenic growth factors. This corresponds with our previous study, where the VEGF concentration

in PL was determined as 5 ng/ml using ELISA (Duttenhoefer et al., 2013), which may be below the detection level of the membrane-based assay used in the current study. Low expression levels of VEGF as well as donor variability have also been shown by others (Lubkowska et al., 2012). Interestingly, certain anti-angiogenic factors, including Timp-1, Timp-2 and endostatin were detected in our PL preparations, although at low levels.

We tested two different PL-containing culture media and directly compared them to EGM containing recombinant growth factors. Considering the functional properties of EPCCs, specifically the uptake of acLDL and tube formation on Matrigel™, EGM showed better results than either PL-containing media. This might be explained by the absence of prominent pro-angiogenic factors such as VEGF as well as the presence of anti-angiogenic factors in PL as discussed above. Thus, we suggest that expansion of EPCCs in the PL-containing medium retains EPCCs in a more immature, progenitor-like state. Nevertheless, our animal study clearly demonstrated that EPCCs grown in PL-containing medium were able to promote the formation of functional capillary-like structures *in vivo*.

EPCC–MSC crosstalk is crucial for neovascularization

In our *in vivo* study, we observed significantly more vessel formation in pre-cultured scaffolds seeded with MSCs and EPCCs in comparison to monocultures. Along with our earlier work, this indicates that interactions of MSCs and EPCCs are required to promote neovascularization. In an earlier study, we studied similar co-cultures *in vitro* and found a more pronounced tube formation in MSC–EPC co-cultures compared to single cultures (Duttenhoefer et al., 2013). We demonstrated the presence of pericytic cells, which have a stabilizing effect on the newly formed vessels. Recent work from our group further showed that a pericyte-like phenotype is induced in MSC–EPCC co-cultures after 3 days and that MSCs are the origin of pericytic cells (Loibl et al., 2014). A direct cell-to-cell contact was crucial to promote the differentiation of MSCs. Similar results were reported by Goerke et al. suggesting that the formation and stabilization of vessels is supported by MSCs, which in presence of EPCs, differentiate towards smooth muscle cells (Goerke et al., 2012). Another study demonstrated a cross-talk between MSCs and EPCs evoking an upregulation of pro-angiogenic factors (Aguirre et al., 2010). This was attributed to both, a direct cell-to-cell contact and paracrine signaling. It has been shown that paracrine signaling involves BMP-2, which in turn upregulates the expression and secretion of angiogenic factors in EPCs (Raida et al., 2006; Nukavarapu and Amini, 2011; Song et al., 2011). The efficient neovascularization that was detected in scaffolds with MSC–EPCC co-cultures might thus be facilitated by both, the formation of stabilizing pericytic cells and by pro-angiogenic factors. Several recent *in vivo* studies confirmed that MSC–EPC interactions facilitate the vessel-formation abilities of EPCs. Fedorovitch et al. showed that addition of MSCs supported the tube formation by blood-derived EPCs in a Matrigel™ plaque assay *in vivo* (Fedorovich et al., 2010). Moreover, co-cultures of MSCs with either blood- or BM-derived EPCs have been shown to promote neovascularization in various bone tissue engineered constructs *in vivo* (Fuchs et al., 2009; Henrich et al., 2009; Pang et al., 2013; Zhang et al., 2012; Seebach et al., 2012). Interestingly in the current study, the beneficial effects of MSC–EPCC co-cultures were only detected in pre-cultured scaffolds. Nevertheless, we could detect vascularization in the center of directly implanted scaffolds. Here, we suggest that the mechanism of neovascularization may be different. In pre-cultured scaffolds the period of *in vitro* culture allows the formation of early tubular structures prior implantation, as previous work has shown (Duttenhoefer et al., 2013). In contrast, in directly implanted scaffolds cells are challenged to the *in vivo* situation in an undifferentiated state. Given the considerable size of scaffolds and the consequent limitations of diffusion of oxygen and nutrients into the scaffold (Folkman and Hochberg, 1973; Auger et al., 2013) it is reasonable to assume that MSCs may not survive in this setting. Additionally, it has been shown that EPCs may adjust to hypoxic conditions (Hoffmann et al., 2013). Further, EPCs may act as a source of chemoattractant factors (Krenning et al., 2009). Taken together this might explain the positive relationship between the number of EPCCs and the number of detected vessels in directly implanted scaffolds.

Conclusions

In conclusion, the current study identifies BM-derived EPCCs as an autologous source of cells with high angiogenic potential. Furthermore, EPCCs preserve their endothelial potential when cultured with platelet-derived autologous growth factors *in vitro* and *in vivo*. Thus, BM-derived EPCCs are a promising source of cells to promote neovascularization in tissue engineered constructs.

Acknowledgments

The authors thank AOER/AO Foundation for funding. The FACS AriaIII was kindly donated by the Innovationsstiftung Graubünden. The authors further wish to thank Dr. L. Benneker for providing BM samples and M. Bluvol, K. Camenisch, S. Peters, M. Glarner and C. Sprecher for technical assistance. The authors wish to thank Dr. J. Bara for proof reading the manuscript.

Appendix A. Supplementary data

Supplementary data to this article can be found online at http://dx.doi.org/10.1016/j.scr.2014.10.005.

References

Aguirre, A., Planell, J.A., Engel, E., 2010. Dynamics of bone marrow-derived endothelial progenitor cell/mesenchymal stem cell interaction in co-culture and its implications in angiogenesis. Biochem. Biophys. Res. Commun. 400 (2), 284–291.

Amini, A.R., Laurencin, C.T., Nukavarapu, S.P., 2012. Differential analysis of peripheral blood- and bone marrow-derived endothelial progenitor cells for enhanced vascularization in bone tissue engineering. J. Orthop. Res. 30 (9), 1507–1515.

Arenberg, D.A., Polverini, P.J., Kunkel, S.L., et al., 1997. In vitro and in vivo systems to assess role of C-X-C chemokines in regulation of angiogenesis. Methods Enzymol. 288, 190–220.

Asahara, T., Murohara, T., Sullivan, A., et al., 1997. Isolation of putative progenitor endothelial cells for angiogenesis. Science 275 (5302), 964–967.

Asahara, T., Masuda, H., Takahashi, T., et al., 1999. Bone marrow origin of endothelial progenitor cells responsible for postnatal vasculogenesis in physiological and pathological neovascularization. Circ. Res. 85 (3), 221–228.

Auger, F.A., Gibot, L., Lacroix, D., 2013. The pivotal role of vascularization in tissue engineering. Annu. Rev. Biomed. Eng. 15, 177–200.

Carano, R.A., Filvaroff, E.H., 2003. Angiogenesis and bone repair. Drug Discov. Today 8 (21), 980–989.

Case, J., Mead, L.E., Bessler, W.K., et al., 2007. Human CD34+ AC133+ VEGFR-2+ cells are not endothelial progenitor cells but distinct, primitive hematopoietic progenitors. Exp. Hematol. 35 (7), 1109–1118.

Chen, J.Y., Feng, L., Zhang, H.L., et al., 2012. Differential regulation of bone marrow-derived endothelial progenitor cells and endothelial outgrowth cells by the Notch signaling pathway. PLoS ONE 7 (10), e43643.

Critser, P.J., Voytik-Harbin, S.L., Yoder, M.C., 2011. Isolating and defining cells to engineer human blood vessels. Cell Prolif. 44 (Suppl. 1), 15–21.

Das, A., Botchwey, E., 2011. Evaluation of angiogenesis and osteogenesis. Tissue Eng. B Rev. 17 (6), 403–414.

Drela, E., Stankowska, K., Kulwas, A., et al., 2012. Endothelial progenitor cells in diabetic foot syndrome. Adv. Clin. Exp. Med. 21 (2), 249–254.

Duttenhoefer, F., Lara de, F.R., Meury, T., et al., 2013. 3D scaffolds co-seeded with human endothelial progenitor and mesenchymal stem cells: evidence of prevascularisation within 7 days. Eur. Cell. Mater. 26, 49–64.

Fayaz, H.C., Giannoudis, P.V., Vrahas, M.S., et al., 2011. The role of stem cells in fracture healing and nonunion. Int. Orthop. 35 (11), 1587–1597.

Fedorovich, N.E., Haverslag, R.T., Dhert, W.J., et al., 2010. The role of endothelial progenitor cells in prevascularized bone tissue engineering: development of heterogeneous constructs. Tissue Eng. A 16 (7), 2355–2367.

Fekete, N., Gadelorge, M., Furst, D., et al., 2012. Platelet lysate from whole blood-derived pooled platelet concentrates and apheresis-derived platelet concentrates for the isolation and expansion of human bone marrow mesenchymal stromal cells: production process, content and identification of active components. Cytotherapy 14 (5), 540–554.

Folkman, J., Hochberg, M., 1973. Self-regulation of growth in three dimensions. J. Exp. Med. 138 (4), 745–753.

Fuchs, S., Ghanaati, S., Orth, C., et al., 2009. Contribution of outgrowth endothelial cells from human peripheral blood on in vivo vascularization of bone tissue engineered constructs based on starch polycaprolactone scaffolds. Biomaterials 30 (4), 526–534.

Gehling, U.M., Ergun, S., Schumacher, U., et al., 2000. In vitro differentiation of endothelial cells from AC133-positive progenitor cells. Blood 95 (10), 3106–3112.

Goerke, S.M., Plaha, J., Hager, S., et al., 2012. Human endothelial progenitor cells induce extracellular signal-regulated kinase-dependent differentiation of mesenchymal stem cells into smooth muscle cells upon cocultivation. Tissue Eng. A 18 (23–24), 2395–2405.

Griffith, L.G., Naughton, G., 2002. Tissue engineering–current challenges and expanding opportunities. Science 295 (5557), 1009–1014.

Henrich, D., Seebach, C., Kaehling, C., et al., 2009. Simultaneous cultivation of human endothelial-like differentiated precursor cells and human marrow stromal cells on beta-tricalcium phosphate. Tissue Eng. C Methods 15 (4), 551–560.

Hoffmann, B.R., Wagner, J.R., Prisco, A.R., et al., 2013. Vascular endothelial growth factor-A signaling in bone marrow-derived endothelial progenitor cells exposed to hypoxia. Physiol. Genomics 45 (21), 1021–1034.

Jianguo, W., Tianhang, L., Hong, Z., et al., 2010. Optimization of culture conditions for endothelial progenitor cells from porcine bone marrow in vitro. Cell Prolif. 43 (4), 418–426.

Johnson, E.O., Troupis, T., Soucacos, P.N., 2011. Tissue-engineered vascularized bone grafts: basic science and clinical relevance to trauma and reconstructive microsurgery. Microsurgery 31 (3), 176–182.

Kalka, C., Masuda, H., Takahashi, T., et al., 2000. Transplantation of ex vivo expanded endothelial progenitor cells for therapeutic neovascularization. Proc. Natl. Acad. Sci. U. S. A. 97 (7), 3422–3427.

Kolbe, M., Dohle, E., Katerla, D., et al., 2010. Enrichment of outgrowth endothelial cells in high and low colony-forming cultures from peripheral blood progenitors. Tissue Eng. C Methods 16 (5), 877–886.

Koob, S., Torio-Padron, N., Stark, G.B., et al., 2011. Bone formation and neovascularization mediated by mesenchymal stem cells and endothelial cells in critical-sized calvarial defects. Tissue Eng. Part A 17 (3–4), 311–321.

Krenning, G., van Luyn, M.J., Harmsen, M.C., 2009. Endothelial progenitor cell-based neovascularization: implications for therapy. Trends Mol. Med. 15 (4), 180–189.

Kuroda, R., Matsumoto, T., Kawakami, Y., et al., 2014. Clinical impact of circulating CD34-positive cells on bone regeneration and healing. Tissue Eng. B Rev. 20 (3), 190–199.

Langer, H.F., May, A.E., Vestweber, D., et al., 2007. Platelet-induced differentiation of endothelial progenitor cells. Semin. Thromb. Hemost. 33 (2), 136–143.

Laroche, M., 2002. Intraosseous circulation from physiology to disease. Joint Bone Spine 69 (3), 262–269.

Laschke, M.W., Harder, Y., Amon, M., et al., 2006. Angiogenesis in tissue engineering: breathing life into constructed tissue substitutes. Tissue Eng. 12 (8), 2093–2104.

Laschke, M.W., Vollmar, B., Menger, M.D., 2009. Inosculation: connecting the life-sustaining pipelines. Tissue Eng. B Rev. 15 (4), 455–465.

Leshem-Lev, D., Omelchenko, A., Perl, L., et al., 2010. Exposure to platelets promotes functional properties of endothelial progenitor cells. J. Thromb. Thrombolysis 30 (4), 398–403.

Lin, Y., Weisdorf, D.J., Solovey, A., et al., 2000. Origins of circulating endothelial cells and endothelial outgrowth from blood. J. Clin. Invest. 105 (1), 71–77.

Lippross, S., Loibl, M., Hoppe, S., et al., 2011. Platelet released growth factors boost expansion of bone marrow derived CD34(+) and CD133(+) endothelial progenitor cells for autologous grafting. Platelets 22 (6), 422–432.

Loibl, M., Binder, A., Herrmann, M., et al., 2014. Direct cell-cell contact between Mesenchymal Stem Cells and Endothelial Progenitor Cells induces a Pericyte-like Phenotype in vitro. Biomed. Res. Int. http://dx.doi.org/10.1155/2014/395781 10.

Lubkowska, A., Dolegowska, B., Banfi, G., 2012. Growth factor content in PRP and their applicability in medicine. J. Biol. Regul. Homeost. Agents 26 (2 Suppl 1), 3S–22S.

Masuda, H., Asahara, T., 2003. Post-natal endothelial progenitor cells for neovascularization in tissue regeneration. Cardiovasc. Res. 58 (2), 390–398.

Mund, J.A., Estes, M.L., Yoder, M.C., et al., 2012. Flow cytometric identification and functional characterization of immature and mature circulating endothelial cells. Arterioscler. Thromb. Vasc. Biol. 32 (4), 1045–1053.

Muscari, C., Gamberini, C., Basile, I., et al., 2010. Comparison between culture conditions improving growth and differentiation

of blood and bone marrow cells committed to the endothelial cell lineage. Biol. Proced. Online 12 (1), 9023.

Nukavarapu, S.P., Amini, A.R., 2011. Optimal scaffold design and effective progenitor cell identification for the regeneration of vascularized bone. Conf. Proc. IEEE Eng. Med. Biol. Soc. 2011, 2464–2467.

Pang, L., Hao, W., Jiang, M., et al., 2013. Bony defect repair in rabbit using hybrid rapid prototyping polylactic-co-glycolic acid/beta-tricalciumphosphate collagen I/apatite scaffold and bone marrow mesenchymal stem cells. Indian J. Orthop. 47 (4), 388–394.

Peichev, M., Naiyer, A.J., Pereira, D., et al., 2000. Expression of VEGFR-2 and AC133 by circulating human CD34(+) cells identifies a population of functional endothelial precursors. Blood 95 (3), 952–958.

Planat-Benard, V., Silvestre, J.S., Cousin, B., et al., 2004. Plasticity of human adipose lineage cells toward endothelial cells: physiological and therapeutic perspectives. Circulation 109 (5), 656–663.

Quirici, N., Soligo, D., Caneva, L., et al., 2001. Differentiation and expansion of endothelial cells from human bone marrow CD133(+) cells. Br. J. Haematol. 115 (1), 186–194.

Rafii, S., Shapiro, F., Rimarachin, J., et al., 1994. Isolation and characterization of human bone marrow microvascular endothelial cells: hematopoietic progenitor cell adhesion. Blood 84 (1), 10–19.

Raida, M., Heymann, A.C., Gunther, C., et al., 2006. Role of bone morphogenetic protein 2 in the crosstalk between endothelial progenitor cells and mesenchymal stem cells. Int. J. Mol. Med. 18 (4), 735–739.

Rouwkema, J., de Boer, J., Van Blitterswijk, C.A., 2006. Endothelial cells assemble into a 3-dimensional prevascular network in a bone tissue engineering construct. Tissue Eng. 12 (9), 2685–2693.

Scherberich, A., Galli, R., Jaquiery, C., et al., 2007. Three-dimensional perfusion culture of human adipose tissue-derived endothelial and osteoblastic progenitors generates osteogenic constructs with intrinsic vascularization capacity. Stem Cells 25 (7), 1823–1829.

Seebach, C., Henrich, D., Wilhelm, K., et al., 2012. Endothelial progenitor cells improve directly and indirectly early vascularization of mesenchymal stem cell-driven bone regeneration in a critical bone defect in rats. Cell Transplant. 21 (8), 1667–1677.

Sekiguchi, H., Ii, M., Jujo, K., et al., 2011. Improved culture-based isolation of differentiating endothelial progenitor cells from mouse bone marrow mononuclear cells. PLoS ONE 6 (12), e28639.

Shi, Y., Kramer, G., Schroder, A., et al., 2014. Early endothelial progenitor cells as a source of myeloid cells to improve the prevascularisation of bone constructs. Eur. Cell. Mater. 27, 64–79.

Song, X., Liu, S., Qu, X., et al., 2011. BMP2 and VEGF promote angiogenesis but retard terminal differentiation of osteoblasts in bone regeneration by up-regulating Id1. Acta Biochim. Biophys. Sin. (Shanghai) 43 (10), 796–804.

Suffee, N., Hlawaty, H., Meddahi-Pelle, A., et al., 2012. RANTES/CCL5-induced pro-angiogenic effects depend on CCR1, CCR5 and glycosaminoglycans. Angiogenesis 15 (4), 727–744.

Thein-Han, W., Xu, H.H., 2013. Prevascularization of a gas-foaming macroporous calcium phosphate cement scaffold via coculture of human umbilical vein endothelial cells and osteoblasts. Tissue Eng. Part A 19 (15–16), 1675–1685.

Timmermans, F., Plum, J., Yoder, M.C., et al., 2009. Endothelial progenitor cells: identity defined? J. Cell. Mol. Med. 13 (1), 87–102.

Tremblay, P.L., Hudon, V., Berthod, F., et al., 2005. Inosculation of tissue-engineered capillaries with the host's vasculature in a reconstructed skin transplanted on mice. Am. J. Transplant. 5 (5), 1002–1010.

Verrier, S., Meury, T.R., Kupcsik, L., et al., 2010. Platelet-released supernatant induces osteoblastic differentiation of human mesenchymal stem cells: potential role of BMP-2. Eur. Cell. Mater. 20, 403–414.

Yang, N., Li, D., Jiao, P., et al., 2011. The characteristics of endothelial progenitor cells derived from mononuclear cells of rat bone marrow in different culture conditions. Cytotechnology 63 (3), 217–226.

Yin, A.H., Miraglia, S., Zanjani, E.D., et al., 1997. AC133, a novel marker for human hematopoietic stem and progenitor cells. Blood 90 (12), 5002–5012.

Yoder, M.C., Mead, L.E., Prater, D., et al., 2007. Redefining endothelial progenitor cells via clonal analysis and hematopoietic stem/progenitor cell principals. Blood 109 (5), 1801–1809.

Yu, H., VandeVord, P.J., Gong, W., et al., 2008. Promotion of osteogenesis in tissue-engineered bone by pre-seeding endothelial progenitor cells-derived endothelial cells. J. Orthop. Res. 26 (8), 1147–1152.

Yu, H., VandeVord, P.J., Mao, L., et al., 2009. Improved tissue-engineered bone regeneration by endothelial cell mediated vascularization. Biomaterials 30 (4), 508–517.

Zhang, R., Gao, Z., Geng, W., et al., 2012. Engineering vascularized bone graft with osteogenic and angiogenic lineage differentiated bone marrow mesenchymal stem cells. Artif. Organs 36 (12), 1036–1046.

Zhao, Y.H., Yuan, B., Chen, J., et al., 2013. Endothelial progenitor cells: therapeutic perspective for ischemic stroke. CNS Neurosci. Ther. 19 (2), 67–75.

Zhou, J., Lin, H., Fang, T., et al., 2010. The repair of large segmental bone defects in the rabbit with vascularized tissue engineered bone. Biomaterials 31 (6), 1171–1179.

Zisch, A.H., 2004. Tissue engineering of angiogenesis with autologous endothelial progenitor cells. Curr. Opin. Biotechnol. 15 (5), 424–429.